nature photonics

LETTERS

PUBLISHED ONLINE: 24 JULY 2011 | DOI: 10.1038/NPHOTON.2011.140

High-energy pulse synthesis with sub-cycle waveform control for strong-field physics

Shu-Wei Huang[1], Giovanni Cirmi[1], Jeffrey Moses[1], Kyung-Han Hong[1], Siddharth Bhardwaj[1], Jonathan R. Birge[1], Li-Jin Chen[1], Enbang Li[2], Benjamin J. Eggleton[2], Giulio Cerullo[3] and Franz X. Kärtner[1,4]*

Over the last decade, control of atomic-scale electronic motion by non-perturbative optical fields has broken tremendous new ground with the advent of phase-controlled high-energy few-cycle pulse sources[1]. The development of close to single-cycle, carrier-envelope phase controlled, high-energy optical pulses has already led to isolated attosecond EUV pulse generation[2], expanding ultrafast spectroscopy to attosecond resolution[1]. However, further investigation and control of these physical processes requires sub-cycle waveform shaping, which has not been achievable to date. Here, we present a light source, using coherent wavelength multiplexing, that enables sub-cycle waveform shaping with a two-octave-spanning spectrum and a pulse energy of 15 μJ. It offers full phase control and allows generation of any optical waveform supported by the amplified spectrum. Both energy and bandwidth scale linearly with the number of sub-modules, so the peak power scales quadratically. The demonstrated system is the prototype of a class of novel optical tools for attosecond control of strong-field physics experiments.

Since the invention of pulsed lasers, the ultrafast laser science community has strived for ever broader optical bandwidths, shorter pulse durations, higher pulse energies and improved phase control. Each breakthrough in generation methods has led to new scientific discoveries in a wide range of fields[3–5]. Recent investigations of phenomena at the intersection of ultrafast and strong-field laser physics, such as high-harmonic generation (HHG)[6] and strong-field ionization[7], have demanded that laser sources combine each of the breakthroughs mentioned above. Investigation and control of the strong-field light–matter interaction simultaneously requires a multi-octave-spanning bandwidth, an isolated sub-cycle waveform, peak intensity above 1×10^{14} W cm^{-2} and full phase control. Such features would allow arbitrary shaping of the strong electric-field waveform for steering ionized electron wave packets[8] and precise control of tunnelling and multi-photon ionization events.

For over two decades, laser scientists have sought to extend laser bandwidths and achieve sub-cycle optical waveforms by synthesizing multiple laser sources[9]. Attempts to combine two independent mode-locked lasers have met with some success, for example in frequency metrology[10,11], but are challenging because of the differential phase noise beyond the achievable feedback loop bandwidth. This problem was recently circumvented by coherently adding two pulse trains derived from the same fibre laser, resulting in the first demonstration of an isolated single-cycle optical pulse source[12]. This proved the feasibility of pulse synthesis at the nanojoule level, but achieving high pulse energy requires the synthesis of low-repetition-rate pulses, which is a challenge because of the environmental perturbations typical of high-energy amplifiers. An approach to high-energy pulse synthesis based on combining the pump, signal and idler of a multi-cycle optical parametric amplifier is being investigated, and shows the potential to produce multiple single-cycle pulses under a multi-cycle envelope with pulse separation on the order of a few femtoseconds[13].

In this Letter, we address the challenge of high-energy sub-cycle optical waveform synthesis. We demonstrate a new approach, based on coherent wavelength multiplexing of ultra-broadband optical parametric chirped pulse amplifiers (OPCPAs), for the generation of fully controlled high-energy non-sinusoidal optical waveforms with spectra spanning close to two octaves. By means of simulation, we present an example of the unique features of our source as a driver for isolated strong-field physics experiments: the confinement of the strong-field light–matter interaction to within an optical cycle and attosecond control of the interaction. The system coherently combines two carrier-envelope phase (CEP)-controlled, few-cycle pulses obtained from different OPCPAs: (i) a near-infrared (NIR) OPCPA, producing 25 μJ, 9 fs pulses centred at 870 nm and (ii) a short-wavelength infrared (SWIR) OPCPA, producing 25 μJ, 24 fs pulses centred at 2.15 μm. The ultra-broadband OPCPA is the most promising technology for producing wavelength-tunable, high-peak-power and high-average-power, few-cycle optical pulses with good pre-pulse contrast[14]. Furthermore, an ultra-broadband OPCPA maintains good CEP stability due to the low thermal load and the small dispersion required to stretch and compress the signals.

Figure 1 shows a schematic of the system. It starts with an actively CEP-stabilized octave-spanning Ti:sapphire oscillator. Using a single oscillator as the front-end for the entire system ensures the coherence of the two OPCPA pulses to within environmental fluctuations and drifts on subsequent beam paths. The designs of the OPCPAs follow the guidelines described in previous studies[15,16] for simultaneously optimizing energy conversion, amplification bandwidth and signal-to-noise ratio. Of note, the inclusion of an acousto-optic programmable dispersive filter (AOPDF) in each OPCPA allows independent spectral phase and amplitude adjustment of each pulse, enabling control and optimization of the synthesized waveform.

Outputs from the two OPCPAs are combined in a broadband neutral beamsplitter. The overall spectrum spans over 1.8 octaves (green lines in Fig. 2a), and the energy of the synthesized pulse is 15 μJ. Besides the spectral phases (controlled by the AOPDFs),

[1]Department of Electrical Engineering and Computer Science and Research Laboratory of Electronics, Massachusetts Institute of Technology, Cambridge, Massachusetts 02139, USA, [2]Centre for Ultrahigh Bandwidth Devices for Optical Systems, Australian Research Council Centre of Excellence, School of Physics, University of Sydney, NSW 2006, Australia, [3]IFN-CNR, Dipartimento di Fisica, Politecnico di Milano, Piazza L. Da Vinci 32, 20133 Milano, Italy, [4]DESY-Center for Free-Electron Laser Science and Hamburg University, Notkestraße 85, D-22607 Hamburg, Germany. *e-mail: kaertner@mit.edu

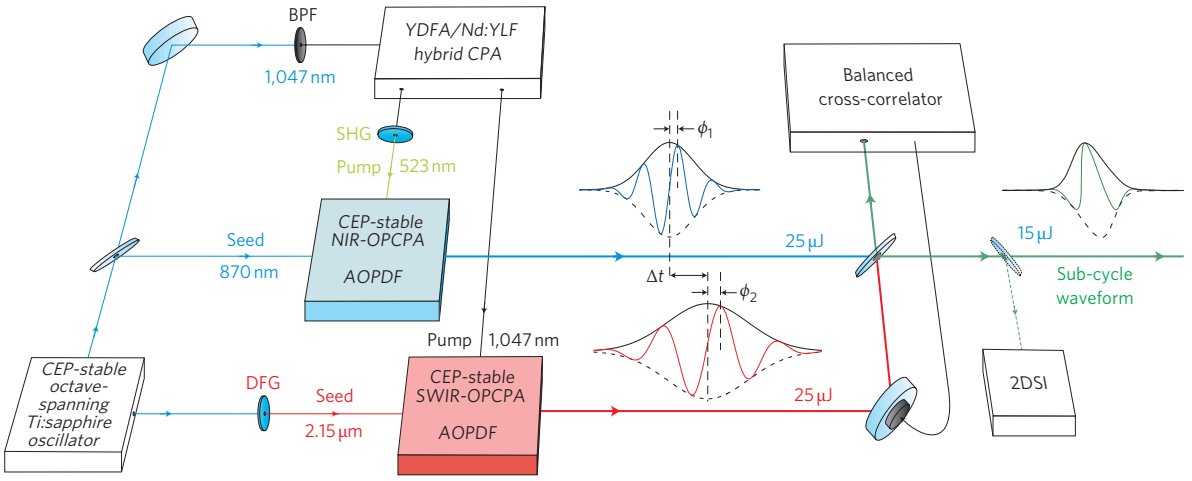

Figure 1 | Schematic of the high-energy optical waveform synthesizer. Two CEP-stabilized, few-cycle OPCPAs centred at different wavelengths are combined based on the concept of coherent wavelength multiplexing to produce a fully controlled non-sinusoidal optical waveform with a pulse energy of 15 μJ at a repetition rate of 1 kHz. Full control over the optical phase allows for any optical waveform given the amplified spectrum. YDFA, ytterbium-doped fibre amplifier; BPF, bandpass filter; DFG, difference frequency generation (intra-pulse).

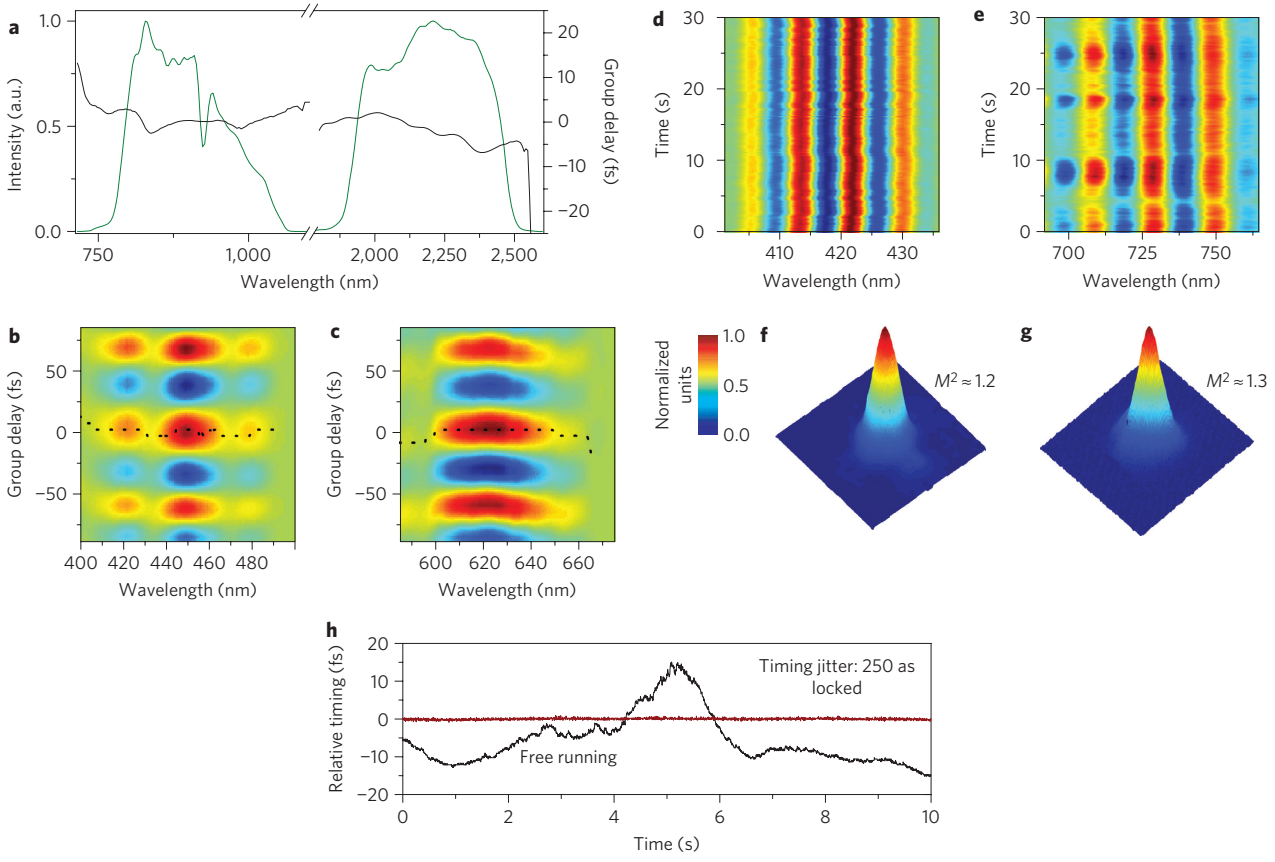

Figure 2 | Characterization of the synthesized pulses. a, Optical spectrum (green) and frequency-dependent group delay (black) of the synthesized pulses. The overall spectrum spans over 1.8 octaves and supports non-sinusoidal waveforms with sub-cycle features. **b**,**c**, 2DSI trace for the NIR OPCPA (**b**) and the SWIR OPCPA (**c**). The 2DSI measurements show that the two pulses are temporally overlapped and well compressed to within 10% of the transform-limited pulse duration. CEP stabilities are verified using nonlinear interferograms with five-shot integration. **d**, *f*–2*f* interferogram, measuring 135 mrad r.m.s. CEP fluctuations over 30 s for the NIR OPCPA. **e**, *f*–3*f* interferogram, measuring 127 mrad r.m.s. CEP fluctuations over 30 s for the SWIR OPCPA. Spatial properties are characterized by measuring the beam profiles and the M^2 values. **f**,**g**, Beam profile of the NIR OPCPA (**f**) and the SWIR OPCPA (**g**). The M^2 value of the NIR-OPCPA is 1.2 and that of the SWIR OPCPA is 1.3. The BCC-assisted feedback loop guarantees the relative timing stability. **h**, BCC measurements of the free-running (black) and closed-loop (red) systems. The closed-loop system ensures a relative timing drift of 250 as, less than 5% of the oscillation period of the SWIR OPCPA (over 10 s).

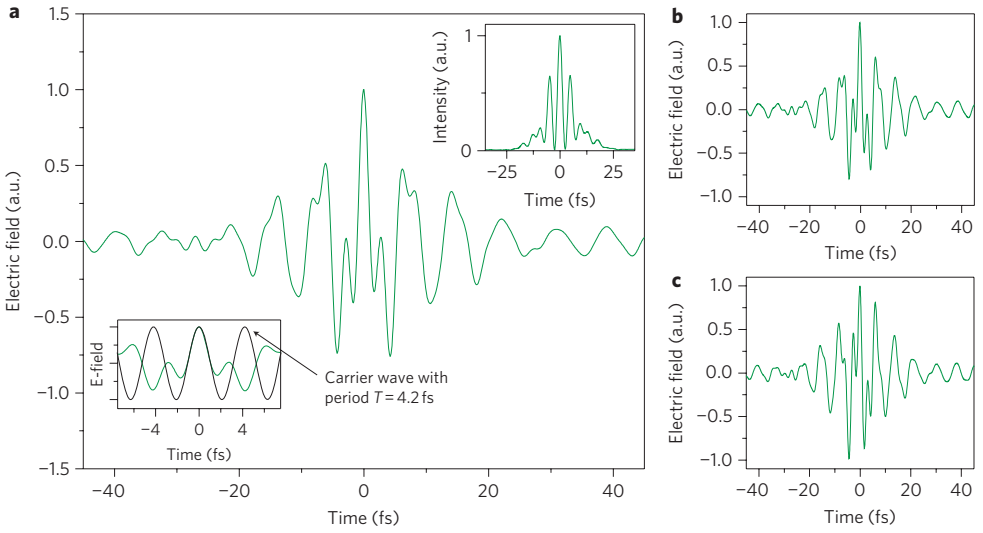

Figure 3 | The synthesized electric-field waveforms. a, Here, we assume CEPs ($\phi_1 = 650$ mrad, $\phi_2 = -750$ mrad) optimal for achieving the shortest high-field transient, which lasts only 0.8 cycles (amplitude FWHM) of the carrier (centroid) frequency. Lower inset: the waveform is plotted in a shorter time window and superimposed with an electric field oscillating at the carrier (centroid) frequency, showing that the synthesized electric-field waveform is non-sinusoidal and the main feature lasts less than an optical cycle. Upper inset: corresponding intensity profile. About one-third of the pulse energy is contained in the main pulse. As an example of waveform shaping made possible by tuning the parameters of our system, two additional atypical waveforms are shown. **b**, A waveform synthesized by adding 500 mrad to both ϕ_1 and ϕ_2. **c**, A waveform synthesized by adding 1 fs to Δt.

three other independent parameters (Fig. 1) determine the synthesized electric-field waveform: the CEP of the NIR OPCPA pulse (ϕ_1), the CEP of the SWIR OPCPA pulse (ϕ_2) and the relative timing between the two OPCPA pulses (Δt). Precise stabilization of these three parameters is required for coherent synthesis of the two OPCPA pulses, and subsequent control of each parameter allows precise waveform shaping. Although the CEP of the SWIR OPCPA is passively stabilized due to the intrapulse difference-frequency generation (DFG)[17] used to produce its seed, an active feedback loop on the oscillator is implemented to ensure the CEP stability of the NIR OPCPA. Figure 2d,e demonstrates the CEP stability of the two individual pulses, with r.m.s. fluctuations as low as 135 mrad and 127 mrad, respectively. Figure 2h characterizes the relative timing stability. A feedback loop based on a balanced cross-correlator (BCC)[18] is implemented to synchronize the two pulses, allowing attosecond-precision relative timing stability. With the feedback control of the SWIR OPCPA's path length over a bandwidth of 30 Hz, the relative timing drift is reduced to 250 as, less than 5% of the oscillation period of the SWIR OPCPA (7.2 fs).

Once the BCC-assisted feedback loop stabilizes the relative timing between the two OPCPA pulses, a two-dimensional spectral-shearing interferometer (2DSI)[19] is used to measure the frequency-dependent group delay of the synthesized pulse. Figure 2b,c presents the raw data of a 2DSI measurement, and Fig. 2a plots (black lines) the extracted frequency-dependent group delay of the synthesized pulse, which is the derivative of the spectral phase with respect to frequency. The 2DSI measurement shows that the two OPCPA pulses are temporally overlapped, and each is well compressed to within 10% of its transform-limited pulse duration.

In our system, the CEPs can be varied by slight tuning of any dispersive element, including the AOPDFs[20]. The values of the CEP will be determined automatically *in situ* when strong-field experiments are conducted[21], so CEP tunability is sufficient from an experimental point of view. In summary, our system is capable of stabilizing and controlling all independent parameters that define the synthesized electric-field waveform. Figure 3a plots a synthesized electric-field waveform and intensity profile assuming the CEPs ($\phi_1 = 650$ mrad, $\phi_2 = -750$ mrad) optimal for achieving the shortest high-field transient, which lasts only 0.8 cycles (amplitude FWHM) of the carrier (centroid) frequency ($\lambda_c = 1.26$ μm). The lower inset of Fig. 3a clearly shows that the synthesized electric-field waveform is non-sinusoidal, and the main feature lasts less than an optical cycle. As an example of waveform shaping made possible by tuning the parameters of our system, Fig. 3b,c shows two atypical waveforms as the CEP and relative timing are changed. Because of the large gap in the combined spectrum, there are wings 4.8 fs from the central peak, as shown in Fig. 3a. As we will show below, for processes initiated by strong-field ionization, these wings have a negligible effect. For more demanding applications, the wings can be suppressed by extension of the coherent wavelength multiplexing scheme to include a third OPCPA, centred at 1.5 μm (ref. 22), to fill the spectral gap. The synthesized waveforms are important for optimizing the HHG process[6], which is, to date, the only demonstrated technique for generating isolated attosecond pulses[2]. As an example, we numerically solve the time-dependent Schrödinger equation (TDSE) for a helium atom in a strong laser field to illustrate a possible use of our source for driving direct isolated soft X-ray pulse generation (Fig. 4). The achievable peak intensity (6×10^{14} W cm^{-2}) is chosen such that the total ionization is below the critical ionization level in helium[23]. With the choice of CEPs as in Fig. 4a, substantial ionization is limited to one optical half-cycle, and an isolated soft X-ray pulse spanning over 250 eV is generated (Fig. 4b,c) without the need for gating techniques[24] or spectral filtering, which typically limit the obtainable bandwidth. Using an additional tin filter, which blocks the strong IR driving field and the nonlinearly chirped low-photon-energy spectral content below 70 eV, leads to an isolated 150 as pulse centred at 200 eV. Of note, the non-sinusoidal electric-field waveform leads to drastically changed electron trajectories (compared to those from a sinusoidal driving field), resulting in corresponding changes in quantum diffusion and atto-chirp, which can be controlled by means of the waveform synthesis parameters (ϕ_1, ϕ_2 and Δt). In this example, quantum diffusion dominates over ionization rate (see Supplementary Information) and effectively eliminates the radiation from long trajectories, resulting in isolated soft X-ray pulse generation solely from short trajectories (Fig. 4b). This gives an example of the capability of our light source

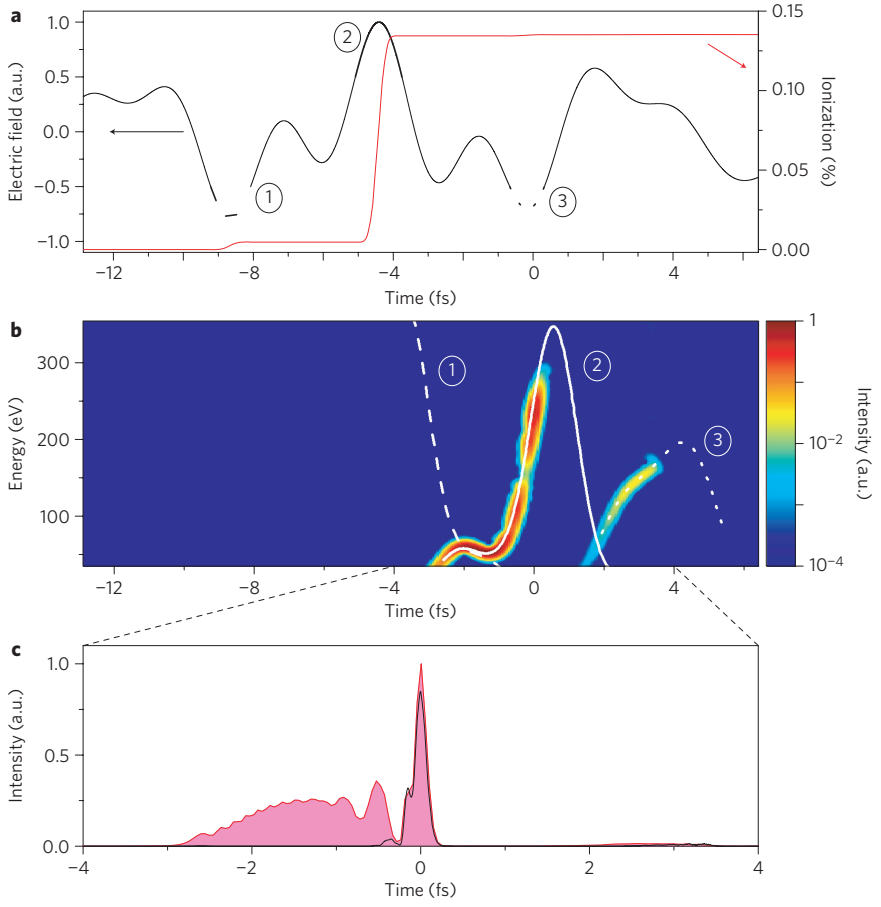

Figure 4 | Extreme nonlinear optics with sub-cycle manipulated waveforms. TDSE simulation results of the single-atom HHG show the uniqueness of our source for direct isolated soft X-ray pulse generation. **a**, Ionization dynamics (red) induced in helium by a linearly polarized electric-field waveform (black) assuming a peak intensity of 6×10^{14} W cm^{-2}, $\phi_1 = 960$ mrad and $\phi_2 = -440$ mrad. **b**, Spectrogram of the HHG superimposed with the calculated classical trajectories. Returning trajectories from three ionization events (2, main pulse; 1 and 3, satellite pulses) are shown for clear interpretation of the spectrogram. The synthesized pulse isolates the ionization process to a half optical cycle, and a continuum spectrum spanning more than 250 eV can be achieved. The isolated soft X-ray pulse has the same sign of chirp over 80% of the spectrum, so the compression setup can be simplified. **c**, Isolated soft X-ray pulse plotted in the time domain before (pink) and after (black line) a 100-nm-thick Sn filter. The Sn filter is chosen for its ability to block the strong IR driving field and the nonlinearly chirped low-photon-energy spectral content, and its good transmission in the soft X-ray range. The filtered isolated soft X-ray pulse has a FWHM duration of 150 as.

to simultaneously isolate the ionization process and manipulate electron trajectories within an optical cycle, allowing unprecedented control of the HHG process.

In conclusion, we have presented a scalable waveform synthesis scheme based on fully controlled coherent wavelength multiplexing of high-energy, few-cycle optical pulses from multi-colour OPCPAs. Currently, the system generates a non-sinusoidal waveform that can be used to drive isolated strong-field physics experiments. The pulse energy is 15 μJ, with the spectrum spanning close to two octaves, and it can be readily scaled both in energy and bandwidth given the proven wavelength tunability of OPCPAs[25] (see Supplementary Information). A numerical study shows the uniqueness of our source for direct isolated soft X-ray pulse generation based on HHG, eliminating the need for gating techniques[24] or spectral filtering. In addition to this application, this new high-intensity laser architecture can be applied to optical field-emission[26], tunnelling ionization studies[27], time-resolved spectroscopy[28] and, in general, attosecond control of strong-field physics experiments.

Methods

OPCPA setup. The system schematic is presented in Supplementary Fig. S1. Both OPCPAs are pumped by an optically synchronized (injection seeded by the Octavius-85M Ti:sapphire oscillator from IdestaQE, Inc.) Nd:YLF chirped pulse amplifier (CPA), which generates 3.5 mJ, 12 ps pulses at 1,047 nm. The SWIR OPCPA, pumped by 1 mJ of the Nd:YLF CPA output, follows the design method in ref. 15. The seed, produced by intrapulse DFG of the oscillator, is first stretched by a bulk silicon block to 5 ps and pre-amplified to 1.5 μJ in the first OPCPA stage using periodically poled lithium niobate (PPLN). The pre-amplified pulse is further stretched to 9.5 ps by an infrared AOPDF, amplified to 25 μJ in periodically poled stoichiometric lithium tantalate (PPSLT), and then compressed to 24 fs in a broadband anti-reflection coated quartz glass block (Suprasil 300). For the NIR OPCPA, a 2 mJ fraction of the Nd:YLF CPA output is frequency-doubled in a lithium triborate (LBO) crystal and used to amplify the oscillator output. The seed is first stretched to 5 ps by a Brewster prism stretcher. The signal is pre-amplified in a double-pass configuration in a type-I, 5-mm-long β-barium borate (BBO) crystal to 2 μJ. The amplified pulse is further stretched to 6.2 ps by an AOPDF and a grating stretcher, amplified to 25 μJ in BBO and then compressed to 9 fs in a Brewster-cut N-LaSF9 block.

Beam combining. The outputs of the two OPCPAs are combined in a broadband neutral beamsplitter, which introduces 25% energy loss. In addition, only half of the synthesized pulse energy is available for experiments, because the other half is directed to the balanced cross-correlator (BCC). Because the pulse energy directed to the BCC is much greater than is needed, a custom-made dichroic mirror can be implemented to improve the experimentally available pulse energy by a factor of 2.5. Thus, in an optimized system, waveform synthesis could be achieved with very low losses.

We chose to combine the two OPCPA pulses in a 'constant waist width' fashion[29], which is inherently compatible with OPCPA configurations. As shown theoretically in ref. 29, the 'constant waist width' configuration offers the unique property that the temporal pulse form remains unchanged upon propagation.

Relative timing stabilization. One part of the combined beam is directed to a BCC (Supplementary Fig. S2), which consists of two nearly identical cross-correlators using 200-μm-thick BBO crystals, phase-matched for sum-frequency generation of 870 nm light and 2.15 μm light. Use of the SWIR OPCPA delay stage and a 4-mm-thick calcium fluoride (CaF_2) window between cross-correlators sets the group delay between pulses to +25 fs in one cross-correlator and −25 fs in the other. An additional 2-mm-thick calcium fluoride window ensures zero group delay ($\Delta t = 0.0$ fs) at the combined output. For deviations from this zero-delay configuration of up to ±20 fs, the photodetector signal is linearly proportional to the time difference and thus can be used as the error signal fed to the loop filter in the feedback system. Furthermore, in the vicinity of the zero crossing, the setup delivers a balanced signal and thus the amplitude noise of each OPCPA output does not affect the detected error signal.

2DSI. In the 2DSI setup (Supplementary Fig. S3), the combined beam is first split by a beam sampler in which the second surface is anti-reflection coated. A copy of the beam (4%) is Fresnel-reflected and only guided via silver mirrors before being mixed in a 40 μm type II BBO. The other copy of the beam (96%) passes through the beam sampler and is highly stretched before being equally split again by a cube beamsplitter, routed to the BBO and mixed with the unchirped pulse. Two collinear, temporally overlapped, but spectrally sheared up-converted pulses are then generated. To observe the interference between the two up-converted pulses, which encodes the spectral group delay information, the delay of one of the highly chirped pulses is scanned over a few optical cycles. The spectrum of the up-converted signal is recorded as a function of this delay, yielding a two-dimensional intensity function that is shown in Fig. 2b,c. The interpretation of the 2DSI data is relatively straightforward; each spectral component is vertically shifted in proportion to its group delay.

It should be noted that we treat the combined beam as a single pulse, and use the 2DSI to retrieve the frequency-dependent group delay of the synthesized pulse, and not just those of the individual OPCPA pulses. That is, we measured the combined beam, not the two OPCPA pulses independently, and the portion mixed with the unchirped pulse is purely derived from the NIR OPCPA such that the measured spectral group delay has a definite reference throughout the whole spectrum from 700 to 2,500 nm. A different relative timing results in a vertical shift of the fringe patterns in Fig. 2b,c.

Received 23 February 2011; accepted 5 June 2011; published online 24 July 2011

References

1. Krausz, F. & Ivanov, M. Attosecond physics. *Rev. Mod. Phys.* **81,** 163–234 (2009).
2. Goulielmakis, E. *et al.* Single-cycle nonlinear optics. *Science* **320,** 1614–1617 (2008).
3. Udem, T., Holzwarth, R. & Hänsch, T. W. Optical frequency metrology. *Nature* **416,** 233–237 (2002).
4. Kienberger, R. *et al.* Atomic transient recorder. *Nature* **427,** 817–821 (2004).
5. Li, C. H. *et al.* A laser frequency comb that enables radial velocity measurements with a precision of 1 cm s^{-1}. *Nature* **452,** 610–612 (2008).
6. Corkum, P. B. Plasma perspective on strong field multiphoton ionization. *Phys. Rev. Lett.* **71,** 1994–1997 (1993).
7. Keldysh, L. V. Ionization in the field of a strong electromagnetic wave. *Sov. Phys. JETP* **20,** 1307–1314 (1965).
8. Chipperfield, L. E., Robinson, J. S., Tisch, J. W. G. & Marangos, J. P. Ideal waveform to generate the maximum possible electron recollision energy for any given oscillation period. *Phys. Rev. Lett.* **102,** 063003 (2009).
9. Hänsch, T. W. A proposed sub-femtosecond pulse synthesizer using separate phase-locked laser oscillators. *Opt. Commun.* **80,** 71–75 (1990).
10. Wei, Z. Y., Kobayashi, Y., Zhang, Z. G. & Torizuka, K. Generation of two-color femtosecond pulses by self-synchronizing Ti:sapphire and Cr:forsterite lasers. *Opt. Lett.* **26,** 1806–1808 (2001).
11. Shelton, R. K. *et al.* Phase-coherent optical pulse synthesis from separate femtosecond lasers. *Science* **293,** 1286–1289 (2001).
12. Krauss, G. *et al.* Synthesis of a single cycle of light with compact erbium-doped fibre technology. *Nature Photon.* **4,** 33–36 (2010).
13. Cerullo, G., Baltuška, A., Mücke, O. D. & Vozzi, C. Few-optical-cycle light pulses with passive carrier-envelope phase stabilization. *Laser Photon. Rev.* **5,** 323–351 (2011).
14. Dubietis, A., Butkus, R. & Piskarskas, A. P. Trends in chirped pulse optical parametric amplification. *IEEE J. Sel. Top. Quantum Electron.* **12,** 163–172 (2006).
15. Moses, J. *et al.* Highly stable ultrabroadband mid-IR optical parametric chirped-pulse amplifier optimized for superfluorescence suppression. *Opt. Lett.* **34,** 1639–1641 (2009).
16. Moses, J., Manzoni, C., Huang, S. W., Cerullo, G. & Kärtner, F. X. Temporal optimization of ultrabroadband high-energy OPCPA. *Opt. Express* **17,** 5540–5555 (2009).
17. Baltuška, A., Fuji, T. & Kobayashi, T. Controlling the carrier-envelope phase of ultrashort light pulses with optical parametric amplifiers. *Phys. Rev. Lett.* **88,** 1339011 (2002).
18. Schibli, T. R. *et al.* Attosecond active synchronization of passively mode-locked lasers by balanced cross correlation. *Opt. Lett.* **28,** 947–949 (2003).
19. Birge, J. R., Crespo, H. M. & Kärtner, F. X. Theory and design of two-dimensional spectral shearing interferometry for few-cycle pulse measurement. *J. Opt. Soc. Am. B* **27,** 1165–1173 (2010).
20. Forget, N., Canova, L., Chen, X., Jullien, A. & Lopez-Martens, R. Closed-loop carrier-envelope phase stabilization with an acousto-optic programmable dispersive filter. *Opt. Lett.* **34,** 3647–3649 (2009).
21. Wittmann, T. *et al.* Single-shot carrier-envelope phase measurement of few-cycle laser pulses. *Nature Phys.* **5,** 357–362 (2009).
22. Mücke, O. D. *et al.* Scalable Yb-MOPA-driven carrier-envelope phase-stable few-cycle parametric amplifier at 1.5 μm. *Opt. Lett.* **34,** 118–120 (2009).
23. Popmintchev, T. *et al.* Phase matching of high harmonic generation in the soft and hard X-ray regions of the spectrum. *Proc. Natl Acad. Sci. USA* **106,** 10516–10521 (2009).
24. Sansone, G. *et al.* Isolated single-cycle attosecond pulses. *Science* **314,** 443–446 (2006).
25. Cerullo, G. & De Silvestri, S. Ultrafast optical parametric amplifiers. *Rev. Sci. Instrum.* **74,** 1–18 (2003).
26. Hommelhoff, P., Kealhofer, C. & Kasevich, M. A. Ultrafast electron pulses from a tungsten tip triggered by low-power femtosecond laser pulses. *Phys. Rev. Lett.* **97,** 247402 (2006).
27. Arissian, L. *et al.* Direct test of laser tunneling with electron momentum imaging. *Phys. Rev. Lett.* **105,** 133002 (2010).
28. Hochstrasser, R. M. Two-dimensional spectroscopy at infrared and optical frequencies. *Proc. Natl Acad. Sci. USA* **104,** 14190–14196 (2007).
29. Zou, Q. H. & Lu, B. Propagation properties of ultrashort pulsed beams with constant waist width in free space. *Opt. Laser Technol.* **39,** 619–625 (2007).

Acknowledgements

This work was supported by the Air Force Office of Scientific Research (grants FA9550-09-1-0212, FA8655-09-1-3101 and FA9550-10-1-0063) and by Progetto Roberto Rocca.

Author contributions

F.X.K., K.H.H., J.M. and S.W.H. conceived the experiment, and carried it out together with G.Ce. and G.Ci.; S.B. provided the TDSE simulation and the spectrogram analysis; J.R.B. provided critical discussion on 2DSI; L.J.C. provided critical help and discussion on the Ti:sapphire oscillator; E.L. and B.J.E. provided the chirped fibre Bragg grating; S.W.H., G.Ci., K.H.H., J.M., F.X.K. and G.Ce. co-wrote the paper. F.X.K. is the senior author of the group and supervised the work.

Additional information

The authors declare no competing financial interests. Supplementary information accompanies this paper at www.nature.com/naturephotonics. Reprints and permission information is available online at http://www.nature.com/reprints. Correspondence and requests for materials should be addressed to F.X.K.